TISSUE ENGINEERING: Part C
Volume 21, Number 1, 2015

DOI: 10.1089/ten.tec.2013.0622

Human Oral Mucosa Tissue-Engineered Constructs Monitored by Raman Fiber-Optic Probe

Alexander Khmaladze, PhD,[1] Shiuhyang Kuo, PhD,[2] Roderick Y. Kim, DDS,[2,3] Robert V. Matthews,[1] Cynthia L. Marcelo, MS, PhD,[3] Stephen E. Feinberg, DDS, MS, PhD,[2,3] and Michael D. Morris, PhD[1]

In maxillofacial and oral surgery, there is a need for the development of tissue-engineered constructs. They are used for reconstructions due to trauma, dental implants, congenital defects, or oral cancer. A noninvasive monitoring of the fabrication of tissue-engineered constructs at the production and implantation stages done in real time is extremely important for predicting the success of tissue-engineered grafts. We demonstrated a Raman spectroscopic probe system, its design and application, for real-time *ex vivo* produced oral mucosa equivalent (EVPOME) constructs noninvasive monitoring. We performed *in vivo* studies to find Raman spectroscopic indicators for postimplanted EVPOME failure and determined that Raman spectra of EVPOMEs preexposed to thermal stress during manufacturing procedures displayed correlation of the band height ratio of CH_2 deformation to phenylalanine ring breathing modes, giving a Raman metric to distinguish between healthy and compromised postimplanted constructs. This study is the step toward our ultimate goal to develop a standalone system, to be used in a clinical setting, where the data collection and analysis are conducted on the basis of these spectroscopic indicators with minimal user intervention.

Introduction

Tissue-engineered oral mucosa is being used for several applications, including clinical transplantation, *in vitro* models for cell–cell and cell–material interactions, and study of cancer and normal tissue.[1] Mucosal grafts are essential for clinical applications in oral and maxillofacial surgery, including dental implants, preprosthetic surgery, and oral reconstructions subsequent to oral cancer, trauma, or congenital defects. Both oral mucosa and skin grafts require harvesting of tissue from secondary sites, resulting in additional donor site morbidity.[2] In addition, because of their different keratinization patterns, split-thickness skin grafts frequently may not have acceptable mechanical properties. They also contain adnexal structures, which may result in hair formation in the mouth.[3] Furthermore, the limited availability of oral mucosa allows for harvesting only a small graft. As a successful solution to these limitations, tissue engineering has been applied to the fabrication of skin and mucosal substitutes.[4–8] An example of such an engineered substitute is the human *ex vivo* produced oral mucosa equivalent (EVPOME).[2,9–11] EVPOMEs are made from primary human oral keratinocytes, which are grown in a serum-free chemically defined culture medium without a feeder layer on human cadaveric acellular dermis, AlloDerm®. These constructs have excellent handling characteristics. Already, they have been used in human clinical trial approved by the US Food and Drug Administration.[11]

A challenge in the production of tissue-engineered constructs is that many or perhaps most of these cell-based products require continuous real-time monitoring to assess the cell metabolic function and viability before release for use in patients. The monitoring is also needed after grafting into patients.[12] Currently, there is a small number of bioanalytical techniques suitable for such monitoring.[13,14] However, these technologies often require sophisticated specimen preparation, are expensive, and invasive.

Previously, we reported a rapid and noninvasive Raman spectroscopic technique for *in vitro* quality monitoring of EVPOMEs during manufacturing and postmanufacturing.[15,16] In this communication, we demonstrate the use of Raman spectroscopy for *in vivo* monitoring of implanted EVPOMEs into severe combined immunodeficiency (SCID) mice by means of Raman failure indicators for classification of compromised and control EVPOMEs. This noninvasive *in vivo* monitoring system can assess the quality of EVPOMEs with minimal user intervention. Because it uses an existing portable Raman system, it may be translatable to a clinical setting for use by oral surgeons and operating room personnel and may provide an efficient and real-time noninvasive evaluation of grafted tissue constructs.

Departments of [1]Chemistry and [2]Oral and Maxillofacial Surgery, School of Dentistry, University of Michigan, Ann Arbor, Michigan.
[3]Department of Surgery, Medical School, University of Michigan, Ann Arbor, Michigan.

Materials and Methods

Oral keratinocyte culture and EVPOME manufacture

Procedures of harvesting human oral mucosal tissue were approved by the University of Michigan Institutional Review Board. The processes for primary human oral keratinocyte culture and EVPOME manufacturing were detailed previously.[2,10] Briefly, trypsin (Sigma) was used to dissociate primary human oral keratinocytes from tissues, and keratinocyte cultures were established in a chemically defined culture medium without serum (EpiLife and EDGS; Invitrogen, Life Technologies) containing 0.06 mM calcium, 25 μg/mL gentamicin, and 0.375 μg/mL fungizone. A 1-cm^2 acellular cadaver dermis (AlloDerm; LifeCell Corporation) was presoaked in 0.05 μg/μL human type IV collagen (Sigma) at 4°C overnight and was seeded with 200K oral keratinocytes to produce EVPOMEs. EVPOMEs were immersed in a medium containing 1.2 mM calcium for 4 days and then for an additional 7 days at an air–liquid phase. Control EVPOMEs were maintained at 37°C. Thermally stressed samples were kept at 43°C overnight on day 9 postseeding for 24 h and switched back to 37°C for 24 h before analysis. One-fifth of EVPOMEs were collected at the 11th day after cell seeding and fixed in 10% formalin. The samples were then processed and stained with hematoxylin and eosin (H&E) by the histology core at the University of Michigan School of Dentistry. The rest of the EVPOME samples were surgically implanted into SCID (7- to 8-week-old) mice.

Mouse surgery for EVPOME grafting and postimplanted histology

The University of Michigan Committee on Use and Care of Animals (UCUCA) approved all animal study protocols. Surgical procedures in our mouse model were detailed in a previous article.[17] Briefly, EVPOMEs were implanted into 7- to 8- week-old SCID mice, strain SCID Hairless Outbred (Charles River Laboratories International, Inc.). EVPOMEs were inserted into dorsal subcutaneous pouches for 1 and 3 weeks before *in vivo* analysis. Mice were anesthetized by inhalation using isoflurane. Betadine (Purdue Products L.P.) was applied to disinfect the mice dorsal skin followed by the injection of analgesic buprenorphine. A 2.0-cm^2 subcutaneous pouch was created to accommodate a 1.0-cm^2 EVPOME. A slightly larger sterilized 0.005-inch-thick silicone sheeting (Specialty Manufacturing) was overlaid on each implanted EVPOME to prevent adherence of the EVPOME to the mouse tissue. The epidermal side of the EVPOME, overlaid with cellular layers, was grafted facing toward the overlaying skin of the pocket. The incision was closed with the Autoclip (Becton Dickinson). Postimplanted EVPOMEs were removed from mice after *in vivo* Raman spectroscopic analysis. The samples were fixed in 10% formalin and then processed and stained with H&E by the histology core at the Dental School, University of Michigan. For immunohistochemistry, the anti-pan keratin antibody (ab8068; Abcam) with a dilution of 1:250 was used, and the signals were detected by DAB Chromagen for 5 min with hematoxylin as counterstaining. Eight mice were used for each batch of EVPOME grafting: four mice for 1-week implantation and four for 3-week implantation. Two control and two thermal stressed EVPOMEs were grafted into SCID mice for 1 and 3 weeks of implantation, respectively.

Raman probe

We employed a custom-designed Raman fiber-optic probe system to collect Raman spectra. The system was detailed previously.[18] Briefly, a diode laser (830 nm wavelength; Innovative Photonic Solutions, Inc.) was used for excitation. The laser light was sent through a 300-μm core fiber into a probe head. The probe head contained focusing optics, which included a number of lenses, mirrors, and filters that were used to focus the laser beam onto a specimen, collect Raman signal, and remove the excitation light from the collected Raman signal. The incident laser power was measured to be $\sim$120 mW at the specimen. Raman signal was collected by the focusing optics and steered into a collection fiber bundle, which consisted of 50 fibers (100 μm core diameter). The fibers were arranged into a circular disc at the probe side and were rearranged into a linear array for the light to be coupled into an integrated Raman spectroscopic system (Rxn1; Kaiser Optical Systems, Inc.). A 50-μm entrance slit was used to obtain the spectral resolution of 7–8 cm^{-1}. A HoloSpec Calibration Accessory (Kaiser Optical Systems, Inc.) was used for calibration of the wavelength scale of the spectrograph as well as the wavelength-dependent response of the detector. We have developed a LabVIEW-based software suite, which was used for data acquisition and dark subtraction/baseline adjustment by a modified polyfit method.[19] All the postprocessing and data analysis were done by using locally written LabVIEW/MATLAB scripts.

Data collection and analysis

Spectroscopic measurements were performed on 24 mice. Before measurements, each mouse was anesthetized. Then, its dorsolateral skin was opened to expose the subcutaneously implanted EVPOME. The silicone sheet was removed. In general, we collected three spectra for each mouse. The acquisition time was 5 min for each spectrum.

Levenberg–Marquardt algorithm (implemented in LabVIEW) was used to fit the Raman bands. We have performed *t*-tests to access the ability of Raman metrics to differentiate between stressed and nonstressed constructs. Differences were considered significant at $p < 0.01$. We have determined a threshold value for the most significant Raman metrics that gave the best separation between nonstressed and stressed EVPOMEs. Specificity and sensitivity were calculated using the standard formula.

Results

Histology analysis of pre- and postimplanted EVPOMEs

The representative preimplanted EVPOME histology pictures are shown in Figure 1. The cellular layers were severely damaged when EVPOMEs were cultured at 43°C for 24 h (Fig. 1, right column). Some residual cells and keratin could still be observed for these thermal stressed EVPOMEs. The H&E histology pictures of postimplanted EVPOMEs are shown in Figure 2. To confirm the presence of keratin structure on postimplanted EVPOMEs, the

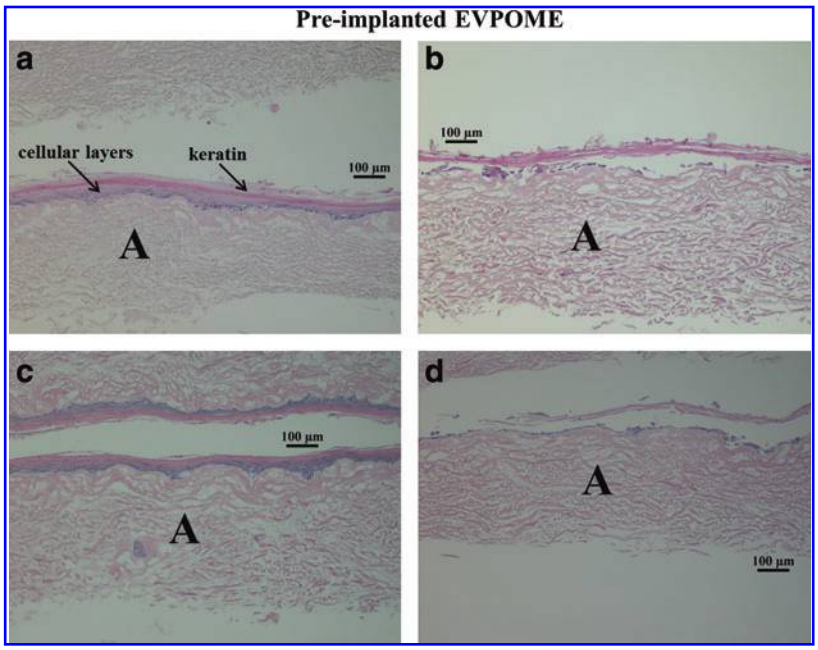

FIG. 1. Representative batch of pre-implanted H&E histology pictures of control **(a, c)** and thermal stressed **(b, d)** EVPOMEs, which were subsequently implanted for 1 week **(a, b)** and 3 weeks **(c, d)**. Thermally stressed specimens were cultured at 43°C for 24 h. Scaffold AlloDerm® areas were marked with ''A.'' All scale bars are 100 μm. EVPOMEs, *ex vivo* produced oral mucosa equivalent; H&E, hematoxylin and eosin. Color images available online at www.liebertpub.com/tec

anti-pan keratin antibody was used and the results are shown in Figure 3. The epithelial layer continued to stratify and differentiate at 1 week postimplantation for control EVPOME (Figs. 2a and 3a, marked with double arrow line). A much lesser degree of reepithelialization was observed on the compromised EVPOME at 1 week postimplantation (Figs. 2b and 3b). At 3 weeks postimplantation, mice cells gradually infiltrated the EVPOMEs and replaced epithelial cells and structure on EVPOMEs. However, much more keratin was left in the control sample due to a higher degree of reepithelialization (Figs. 2c and 3c) when compared with the compromised EVPOME (Figs. 2d and 3d), on which only residual keratin was observed.

In vivo *Raman spectra data analysis*

Representative Raman spectra of thermal stressed and nonstressed EVPOMEs (constructs for 1 and 3 weeks postimplantation) are shown in Figure 4. The phenylalanine band was sharp and contained no unresolved components, which allowed a relatively straightforward peak fitting and thus was convenient to use for normalization of

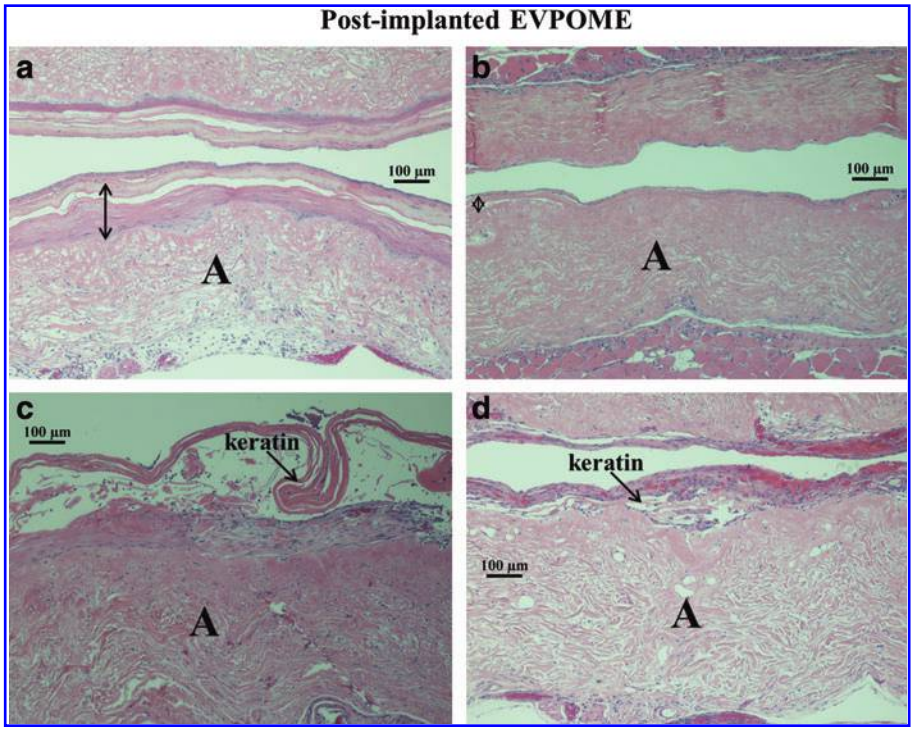

FIG. 2. Representative batch of postimplanted H&E histology pictures of control **(a, c)** and thermal stressed **(b, d)** EVPOMEs, which were implanted for 1 week **(a, b)** and 3 weeks **(c, d)**. Thermally stressed specimens were cultured at 43°C for 24 h. Scaffold AlloDerm areas were marked with ''A.'' Double arrow lines marked the regions of reepithelialization for 1 week postimplanted controls and thermal stressed EVPOMEs. The remaining keratin was marked with arrows on both control and thermal stressed 3 weeks postimplanted EVPOMEs. All scale bars are 100 μm. Color images available online at www.liebertpub.com/tec

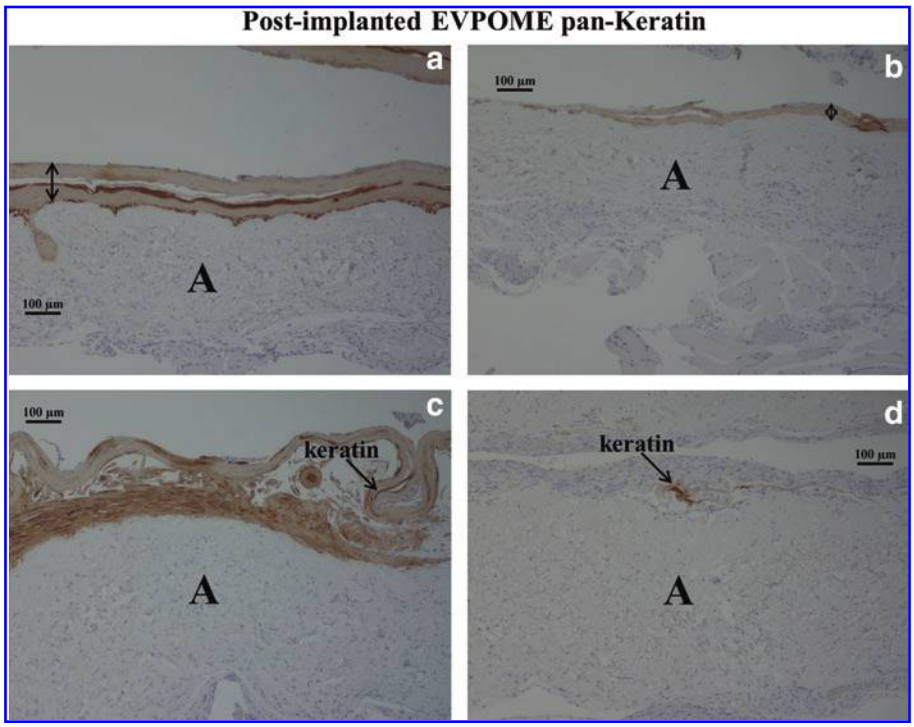

FIG. 3. Representative batch of postimplanted immunohistochemistry histology pictures using anti-pan keratin antibody for control **(a, c)** and thermal stressed **(b, d)** EVPOMEs, which were implanted for 1 week **(a, b)** and 3 weeks **(c, d)**. Thermally stressed specimens were cultured at 43°C for 24 h. Scaffold AlloDerm areas were marked with ''A.'' Double arrow lines marked the regions of reepithelialization for 1 week postimplanted control and thermal stressed EVPOMEs. All scale bars are 100 µm. Color images available online at www.liebertpub.com/tec

spectra. Similar to the *in vitro* measurements,[16] amide III envelope (maximum at 1250 cm^{-1}) and CH_2 deformation (at 1450 cm^{-1}) were clearly identifiable in all the spectra. Multiple overlapping unresolved bands were present in both the amide bands. As Figure 4 shows, changes in shape in the amide III band occurred as a result of thermal stress. The height of CH_2 deformation band (relative to phenylalanine band) also changed. Figure 5 shows the CH_2/phenylalanine band ratios for thermal stressed and nonstressed EVPOMEs for 1 and 3 weeks postimplantation. As Figure 5 demonstrates, the metric (previously developed for the EVPOME constructs investigated *in vitro*[15]) can be used to distinguish between both stressed and nonstressed constructs ($p < 0.001$). There is also a noticeable change between 1 and 3 weeks postimplantation EVPOME ($p = 0.002$).

Furthermore, we examined the CH_2/phenylalanine band height ratio and determined the threshold values that maximize the sensitivity and specificity. By setting the threshold to 6.2 for 1 week postimplantation EVPOMEs and to 4.7 for 3 weeks postimplantation EVPOMEs, the specimens were classified with 92% sensitivity and 93% specificity and

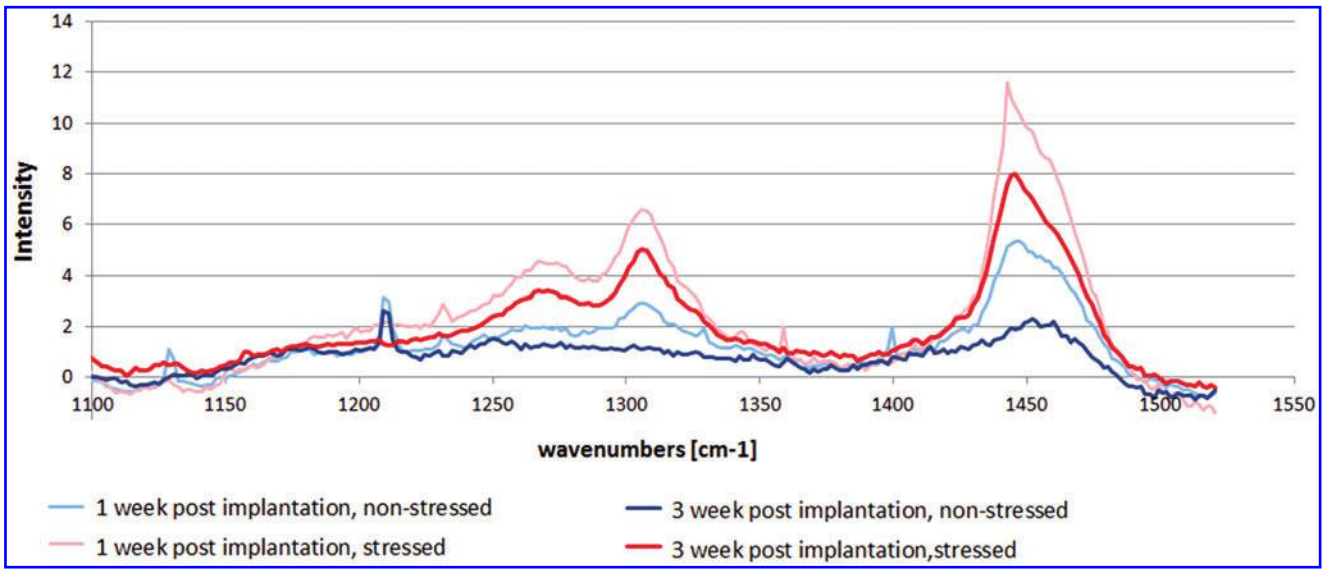

FIG. 4. Raman spectra of thermal stressed and nonstressed EVPOME (implanted in a mouse for 1 and 3 weeks) were normalized to a phenylalanine (1004 cm^{-1}) band. Broad amide III band at 1250 cm^{-1} and CH_2 peak at 1450 cm^{-1} are clearly visible. Color images available online at www.liebertpub.com/tec

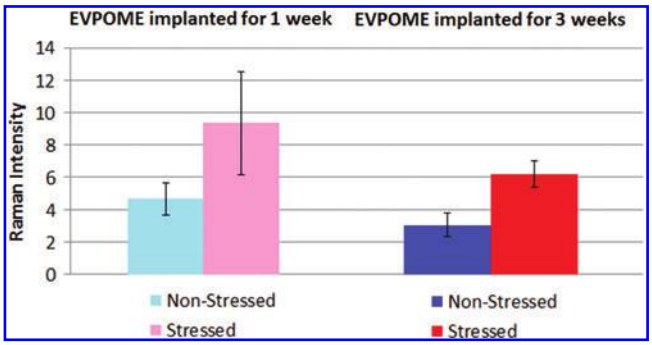

FIG. 5. The ratio of CH_2 to phenylalanine peak heights for stressed and nonstressed EVPOMEs 1 and 3 weeks postimplantation. Each column is based on 15 spectra and error bars are equal to one standard deviation. Color images available online at www.liebertpub.com/tec

100% sensitivity and 94% specificity for 1 week and 3 weeks postimplantation, respectively.

Discussion

As reported previously,[20] structural changes in both EVPOME and AlloDerm® are caused by thermal stress. As the histology data suggest, the disruption of a cell layer was at least partially responsible for the difference between stressed and nonstressed and preimplantation EVPOMEs. The intact and healthy keratinocytes on the epithelial layer of EVPOME could explain the much higher activity of keratinocytes, both in proliferation and in differentiation in control EVPOMEs compared with the thermal stressed ones at 1 week postimplantation. This major structure difference in reepithelialization between the control and compromised implanted EVPOMEs could cause shape changes in the amide envelopes as well as the height of the CH_2 deformation band when measured *in vivo* by Raman spectra. We also surmise that as the implantation time of EVPOMEs increased, the host mice cells played more prominent roles than EVPOMEs themselves, resulting in spectral changes we observed. EVPOMEs with healthy and intact epithelial layers would recruit more host cells to be intergraded into and onto grafts and have more epithelial structures left when compared with compromised or nonhealthy EVPOMEs at 3 weeks postimplantation. The recruitment of more host cells was possibly from the secretion of chemokines, such as IL8, by epithelial cells on EVPOMEs. Our unpublished data indicated that IL8 as a potential candidate to promote the wound healing process of grafted tissue-engineered constructs. Interestingly, Yoshizawa *et al.*[21] also observed similar histology results to our postimplantation EVPOMEs.

The Raman metric, which we originally developed for the *in vitro* measurements, can be applied *in vivo*, as it is capable of distinguishing between grafted stressed and nonstressed EVPOME constructs. By using this ratio, we can determine which constructs are more viable and, thus, noninvasively monitor the postgrafted outcomes in a real time. Also, the noticeable change between 1 and 3 weeks postimplantation EVPOMEs shows that the protein (and possibly lipid content changes) occurring during the implantation can also be detected.

Conclusion

We have developed a fiber-optic probe to investigate EVPOME constructs implanted in mice by examining their Raman spectra. Furthermore, we defined criteria to noninvasively determine the viability of EVPOMEs *in vivo*, which was found to be consistent with the previously reported *in vitro* data.

Based on these intensity ratios, we developed a Raman metric and determined its threshold value, at which the constructs become nonviable. Therefore, by using this metric, we can judge the viability of EVPOME without knowing *a priori* whether or not it was thermally stressed. We have also determined that, in at least some cases, the constructs become nonviable before the changes become visible through histological examination. We conclude that the observed changes in Raman spectra result primarily from heat denaturation of proteins in both the EVPOME constructs and the AlloDerm substrates.

We are now ready to proceed to clinical studies and to noninvasively monitor the implantation of EVPOMEs in human patients. Ultimately, if it is possible to detect that the overall health of a graft appears to be compromised, with Raman spectroscopy, before it is evident clinically, that is, color and texture during physical examination, appropriate therapeutic measures can be taken to salvage the graft before clinical failure, thus saving the patient the cost and time to repeat the procedure. The eventual goal of this project is to design a stand-alone system, which can be used in a clinical setting by surgeons and operating room personnel. Such a system will improve graft management and surveillance, thus supporting novel methods for oral and maxillofacial reconstruction in the future.

Acknowledgments

This work is supported, in part, by NIH Grant R01 DE019431-01. The authors thank Dr. Hiroko Kato for her assistance in mice surgery and Dr. Paul Okagbare for his assistance in initial system setup.

This article expands on work previously reported in SPIE Proceeding paper,[20] as allowed under the copyright policy of SPIE.

Disclosure Statement

No competing financial interests exist.

References

1. Moharamzadeh, K., Colley, H., Murdoch, C., Hearnden, V., Chai, W.L., Brook, I.M., Thornhill, M.H., and MacNeil, S. Tissue-engineered Oral Mucosa. J Dent Res **91,** 642, 2012.
2. Izumi, K., Feinberg, S.E., Iida, A., and Yoshizawa, M. Intraoral grafting of an *ex vivo* produced oral mucosa equivalent: a preliminary report. Int J Oral Maxillofac Surg **32,** 188, 2003.
3. Martis, C. Mucosa versus skin grafts. In: Stoelinga, P.J.W., ed. Proceedings, Consensus conference: The Relative Roles of Vestibuloplasty and Ridge Augmentation in the Management of the Atrophic Mandible. Chicago: Quintessence, 1984, p. 41.
4. Phillips, T.J. New skin for old. Arch Dermatol **134,** 344, 1998.

5. De Luca, M., Albanese, E., Megna, M., Cancedda, R., Mangiante, P.E., Cadoni, A., and Franzi, A.T. Evidence that human oral epithelium reconstituted *in vitro* and transplanted onto patients with defects in the oral mucosa retains properties of the original donor site. Transplantation **50,** 454, 1990.
6. Omura, S., Mizuki, N., Horimoto, S., Kawabe, R., and Fujita, K. A newly developed collagen/silicone bilayer membrane as a mucosal substitute: a preliminary report. J Oral Maxillofac Surg **35,** 85, 1997.
7. Raghoebar, G.M., Tompson, A.M., Scholma, J., Blaauw, E.H., Witjes, M.J.H., and Vissink, A. Use of cultured mucosal grafts to cover defects caused by vestibuloplasty: an *in vitro* study. J Oral Maxillofac Surg **53,** 872, 1995.
8. Tsai, C.-Y., Ueda, M., Hata, K., Horie, K., Hibino, Y., Sugimura, Y., Toriyama, K., and Totii, S. Clinical results of cultured epithelial cell grafting in the oral and maxillofacial region. J Craniomaxillofac Surg **25,** 4, 1997.
9. Izumi, K., Song, J., and Feinberg, S.E. Development of a tissue-engineered human oral mucosa: from the bench to the bed side. Cells Tissues Organs **176,** 134, 2004.
10. Izumi, K., Terashi, H., Marcelo, C.L., and Feinberg, S.E. Development and characterization of a tissue-engineered human oral mucosa equivalent produced in a serum-free culture system. J Dent Res **79,** 798, 2000.
11. Izumi, K., Neiva, R., and Feinberg, S.E. Intraoral grafting of a tissue engineered human oral mucosa. Oral Craniofac Tissue Eng **1,** 103, 2011.
12. MacKay, G. Bioactive wound healing, bioaesthetics and biosurgery: three pillars of product development. Regen Med **1,** 169, 2006.
13. Sun, W., Xu, R., Hu, W., Jin, J., Crellin, H.A., Bielawski, J., Szulc, Z.M., Thiers, B.H., Obeid, L.M., and Mao, C. Upregulation of the human alkaline ceramidase 1 and acid ceramidase mediates calcium-induced differentiation of epidermal keratinocytes. J Invest Dermatol **128,** 389, 2008.
14. Stabler, C.L., Long, R.C., Sambanis, A., and Constantinidis, I. Noninvasive measurement of viable cell number in tissue-engineered constructs in-vitro, using 1H nuclear magnetic resonance spectroscopy. Tissue Eng **11,** 404, 2005.
15. Khmaladze, A., Ganguly, A., Raghavan, M., Kuo, S., Cole, J.H., Marcelo, C.L., Feinberg, S.E., Izumi, K., and Morris, M.D. Raman spectroscopic analysis of human tissue engineered mucosa constructs (EVPOME) perturbed by physical and biochemical methods. Proc SPIE **8219,** 82190J, 2012.
16. Khmaladze, A., Ganguly, S., Kuo, M., Raghavan, R., Kainkaryam, M., Cole, J.H., Marcelo, C.L., Feinberg, S.E., Izumi, K., and Morris, M.D. Examination of human tissue engineered oral mucosa constructs by raman spectroscopy. Tissue Eng C **19,** 299, 2013.
17. Izumi, K., Feinberg, S.E., Terashi, H., and Marcelo, C.L. Evaluation of transplanted tissue-engineered oral mucosa equivalents in severe combined immunodeficient mice. Tissue Eng **9,** 163, 2003.
18. Okagbare, P.I., Begun, D., Tecklenburg, M., Awonusi, A., Goldstein, S.A., and Morris, M.D. Noninvasive Raman spectroscopy of rat tibiae: approach to *in vivo* assessment of bone quality. J Biomed Opt **17,** 090502, 2012.
19. Lieber, C.A., and Mahadevan-Jansen, A. Automated method for subtraction of fluorescence from biological raman spectra. Appl Spectrosc **57,** 1363, 2003.
20. Khmaladze, A., Kuo, S., Okagbare, P.I., Marcelo, C.L., Feinberg, K., and Morris, M.D. Raman fiberoptic probe for monitoring human tissue engineered oral mucosa constructs. Proc SPIE **8579,** 85790L, 2013.
21. Yoshizawa, M., Koyama, T., Kojima, T., Kato, H., Ono, Y., and Saito, C. Keratinocytes of Tissue-engineered human oral mucosa promote re-epithelialization after intraoral grafting in athymic mice. J Oral Maxillofac Surg **70,** 1199, 2012.

Address correspondence to:
Michael D. Morris, PhD
Department of Chemistry
School of Dentistry
University of Michigan
930 N. University Avenue
Ann Arbor, MI 48109-1055

E-mail: mdmorris@umich.edu

Received: October 7, 2013
Accepted: April 24, 2014
Online Publication Date: July 3, 2014

This article has been cited by:

1. Katherine J. I. Ember, Marieke A. Hoeve, Sarah L. McAughtrie, Mads S. Bergholt, Benjamin J. Dwyer, Molly M. Stevens, Karen Faulds, Stuart J. Forbes, Colin J. Campbell. 2017. Raman spectroscopy and regenerative medicine: a review. *npj Regenerative Medicine* **2**:1. . [Crossref]
2. Shiuhyang Kuo, Hyungjin Myra Kim, Zhifa Wang, Eve L. Bingham, Atsuko Miyazawa, Cynthia L. Marcelo, Stephen E. Feinberg. 2017. Comparison of two decellularized dermal equivalents. *Journal of Tissue Engineering and Regenerative Medicine* **83**. . [Crossref]
3. Mads S. Bergholt, Michael B. Albro, Molly M. Stevens. 2017. Online quantitative monitoring of live cell engineered cartilage growth using diffuse fiber-optic Raman spectroscopy. *Biomaterials* . [Crossref]
4. Roderick Youngdo Kim, Sam Seoho Bae, Stephen Elliott Feinberg. 2017. Soft Tissue Engineering. *Oral and Maxillofacial Surgery Clinics of North America* **29**:1, 89-104. [Crossref]
5. Keyvan Moharamzadeh, Helen Colley, Vanessa Hearnden, Craig Murdoch. Tissue-engineered models of oral soft tissue diseases 245-255. [Crossref]
6. Dimitris Gorpas, Dinglong Ma, Julien Bec, Diego R. Yankelevich, Laura Marcu. 2016. Real-Time Visualization of Tissue Surface Biochemical Features Derived From Fluorescence Lifetime Measurements. *IEEE Transactions on Medical Imaging* **35**:8, 1802-1811. [Crossref]
7. Joseph E. Cillo, David Basi, Zachary Peacock, Tara Aghaloo, Gary Bouloux, Thomas Dodson, Sean P. Edwards, Deepak Kademani. 2016. Proceedings of the American Association of Oral and Maxillofacial Surgeons 2015 Research Summit. *Journal of Oral and Maxillofacial Surgery* **74**:3, 429-437. [Crossref]